Integrated Systems and Technologies

Cancer Research

Aberrant Lipid Metabolism in Hepatocellular Carcinoma Revealed by Plasma Metabolomics and Lipid Profiling

Andrew D. Patterson[1], Olivier Maurhofer[2], Diren Beyoğlu[2], Christian Lanz[2], Kristopher W. Krausz[1], Thomas Pabst[3], Frank J. Gonzalez[1], Jean-François Dufour[2,4], and Jeffrey R. Idle[1,2,4]

Abstract

There has been limited analysis of the effects of hepatocellular carcinoma (HCC) on liver metabolism and circulating endogenous metabolites. Here, we report the findings of a plasma metabolomic investigation of HCC patients by ultraperformance liquid chromatography-electrospray ionization-quadrupole time-of-flight mass spectrometry (UPLC-ESI-QTOFMS), random forests machine learning algorithm, and multivariate data analysis. Control subjects included healthy individuals as well as patients with liver cirrhosis or acute myeloid leukemia. We found that HCC was associated with increased plasma levels of glycodeoxycholate, deoxycholate 3-sulfate, and bilirubin. Accurate mass measurement also indicated upregulation of biliverdin and the fetal bile acids 7α-hydroxy-3-oxochol-4-en-24-oic acid and 3-oxochol-4,6-dien-24-oic acid in HCC patients. A quantitative lipid profiling of patient plasma was also conducted by ultraperformance liquid chromatography-electrospray ionization-triple quadrupole mass spectrometry (UPLC-ESI-TQMS). By this method, we found that HCC was also associated with reduced levels of lysophosphocholines and in 4 of 20 patients with increased levels of lysophosphatidic acid [LPA(16:0)], where it correlated with plasma α-fetoprotein levels. Interestingly, when fatty acids were quantitatively profiled by gas chromatography-mass spectrometry (GC-MS), we found that lignoceric acid (24:0) and nervonic acid (24:1) were virtually absent from HCC plasma. Overall, this investigation illustrates the power of the new discovery technologies represented in the UPLC-ESI-QTOFMS platform combined with the targeted, quantitative platforms of UPLC-ESI-TQMS and GC-MS for conducting metabolomic investigations that can engender new insights into cancer pathobiology. *Cancer Res; 71(21); 6590–600. ©2011 AACR.*

Introduction

Hepatocellular carcinoma (HCC) is the fifth commonest and one of the deadliest cancers, with about 50% of cases occurring in China (1–3). The advent of HCC is accompanied by metabolic changes in the liver that are reflected in changes in gene expression, microRNA profiles, together with altered circulating protein and small metabolite concentrations. A considerable number of gene expression studies have been undertaken (4–10) targeted at understanding the progression of HCC, in particular, in relation to hepatitis B virus (HBV) and hepatitis C virus (HCV) infection and also mouse models of HCC. There is virtually no mention in these studies of genes involved in metabolism of small (<1 kDa) cellular metabolites.

Metabolomics involves the global and unbiased definition of the complement of small molecules in a biofluid, tissue, organ, or organism (11–14). To accomplish the goals of a metabolomic study, several different analytic platforms may be required to achieve maximum coverage of the metabolome, and these might include ultraperformance liquid chromatography-electrospray ionization-quadrupole time-of-flight mass spectrometry (UPLC-ESI-QTOFMS) directly on urine or plasma and gas chromatography-mass spectrometry (GC-MS) after extraction of analytes and chemical derivatization. Each platform can produce complementary findings on the same sample sets (15, 16). Molecules bearing formal charges, such as phospholipids, cannot be analyzed directly by GC-MS, but UPLC-ESI-QTOFMS provides an ideal solution. Conversely, neutral lipids, such as free fatty acids and their glycerol and cholesterol esters, are ideally suited to GC-MS analysis after appropriate chemical derivatization. Metabolomic analyses can produce data matrices with millions of individual data points, even with modest numbers of samples. To separate 2 classes, such as HCC and controls, multivariate data analysis is used with unsupervised principal components analysis (PCA)

Authors' Affiliations: [1]Laboratory of Metabolism, Center for Cancer Research, National Cancer Institute, NIH, Bethesda, Maryland; [2]Hepatology Research Group, Department of Clinical Research, University of Bern; [3]University Clinic for Medical Oncology; and [4]University Clinic for Visceral Surgery and Medicine, Inselspital, Bern, Switzerland

Note: Supplementary data for this article are available at Cancer Research Online (http://cancerres.aacrjournals.org/).

Current address for A.D. Patterson: Department of Veterinary and Biomedical Sciences and The Center for Molecular Toxicology and Carcinogenesis, The Pennsylvania State University, University Park, PA 16802.

Corresponding Author: Jeffrey R. Idle, Hepatology Research Group, Department of Clinical Research, University of Bern, Murtenstrasse 35, 3010 Bern, Switzerland. Phone: 41-31-632-87-29; Fax: 41-31-632-49-97; E-mail: jeff.idle@ikp.unibe.ch

doi: 10.1158/0008-5472.CAN-11-0885

and supervised projection to latent structures discriminant analysis (PLS-DA) and random forests machine learning algorithm (17). These methodologies have been used noninvasively to understand the global impact on metabolism in a mouse model of alcohol-induced liver disease (18).

A small number of metabolomic studies on HCC have been reported to date (19–21), and these have been restricted to Chinese patients. Here, we describe a metabolomic study of HCC using UPLC-ESI-QTOFMS combined with chemometric analysis and enhanced by lipid profiling using ultraperformance liquid chromatography-electrospray ionization-triple quadrupole mass spectrometry (UPLC-ESI-TQMS) for quantitation of lysophosphocholines (LPC) and GC-MS for determination of free and esterified fatty acids. A number of both upregulated and downregulated molecules of interest are described for HCC that lead to enhanced understanding of the pathobiology of the disease.

Materials and Methods

Patients

A summary of the study groups is displayed in Table 1. HCC patients ($n = 20$) were those who had been selected for transarterial chemoembolization and, with one exception, were all patients with liver cirrhosis (LC) with confirmed HCC according to European Association for the Study of the Liver (EASL) criteria (22). They comprised 17 males and 3 females with a median age of 61 (mean ± SD = 61.1 ± 11.2) years. Six patients had alcohol-related liver disease, 3 had HBV-related disease, 5 had HCV-related hepatitis, 3 had nonalcoholic steatohepatitis, 1 had nonalcoholic steatohepatitis/alcoholic steatohepatitis, and 2 had hereditary hemochromatosis. The Barcelona-Clinic Liver Cancer staging classifications (23) were 3 stage A, 11 stage B, 5 stage C, and 1 stage D. The Child–Pugh scores were 5 to 6 for 16 patients, with 2 patients with a score of 7, 1 patient with a score of 11, and 1 patient was noncirrhotic. Fifteen patients had Eastern Cooperative Oncology Group scores of 0, and 3 of 1; 2 patients were not scored. They had a median number of nodules of 3 (1–6), with a mean diameter of the largest nodule of 4.7 ± 3.0 cm. Bilirubin levels were 30.6 ± 29.1 (9–120) μmol/L, trough albumin levels were 34.2 ± 4.4 (24–42) g/L, peak international normalized ratio values were 1.20 ± 0.13 (1–1.54), aspartate aminotransferase (AST) of 80.2 ± 56.5 (25–237) U/L, alanine aminotransferase (ALT) of 52.4 ± 34.1 (17–152) U/L, alkaline phosphatase (ALP) of 110 ± 48 (49–233) U/L, γ-glutamyltranspeptidase (GGT) of 260 ± 330 (27–1,504) U/L, and median α-fetoprotein (AFP) concentration was 43.3 [1.3-67,725] ng/mL. Only 10 HCC patients had AFP values above a threshold of 50 ng/ml.

As the first control group, patients with clinically (based on decompensation) or histologically proven liver cirrhosis (LC, $n = 7$), enrolled in surveillance program for HCC and with a negative diagnosis for HCC, were enrolled. They comprised 3 males and 4 females with a median age of 48 (50.3 ± 5.7) years. Six patients had a Child–Pugh score of 5 and 1 had a score of 10, similar to the HCC patient group. Their median AFP concentration was 4.0 (1.4–7.5), and all were well under the threshold of 50 ng/mL.

As a second control group, patients with a diagnosis of acute myelogenous leukemia (AML; $n = 22$) were enrolled, representing another cancer group but without hepatic involvement. They comprised 9 males and 13 females and had a median age of 62 (57.2 ± 13.1) years. Their liver function tests (LFT) were generally within normal ranges and were as follows: bilirubin (10.1 ± 6.5 μmol/L), AST (37.2 ± 19.9 U/L), ALT (48.0 ± 38.0 U/L), ALP (161 ± 175 U/L), GGT (208 ± 291 U/L).

Table 1. Demographics and clinical measurements of study groups

	HCC	LC	AML	Healthy volunteers
Age, y	61.1 ± 11.2	50.3 ± 5.7	57.2 ± 13.1	47.0 ± 10.7
Gender	17 M/3 F	3 M/4 F	9 M/13 F	6 M
Child–Pugh score (No. of patients)	5 (10) 6 (6) 7 (2) 11 (1) Noncirrhotic (1)	5 (6) 10 (1)	—	—
AFP (range), ng/mL	3,663 ± 15,087 (1.3–67,725)	4.0 ± 2.0 (1.4–7.5)	—	—
ALT, U/L	52.4 ± 34.1	44.0 ± 31.1	48.0 ± 38.0	—
AST, U/L	80.2 ± 56.5	59.0 ± 37.7	37.2 ± 19.9	—
ALP, U/L	110 ± 48	130 ± 127	161 ± 175	—
GGT, U/L	260 ± 330	126 ± 111	208 ± 291	—
Bilirubin, μmol/L	30.6 ± 29.1	17.0 ± 14.3	10.0 ± 6.5	—

NOTE: All values are expressed as the average ± SD.
Abbreviations: F, female; M, male; —, measurement not conducted.

Finally, a third control group of male healthy volunteers (HV, $n = 6$) were enrolled. They had a median age of 47.5 (49.0 ± 10.6) years. ANOVA revealed no statistically significant differences in age between any of the 4 study groups.

All subjects provided written informed consent before enrollment into the study. The study was approved by the Institutional Review Board and complied with the provisions of the Good Clinical Practice Guidelines and the Declaration of Helsinki and local laws.

Compounds

Butylated hydroxytoluene (BHT) was obtained from Merck Schuchardt OHG. The following LPCs and lysophosphatidic acids (LPA) were obtained from Avanti Polar Lipids, Inc.: LPC (14:0/0:0), LPC(15:0/0:0), LPC(16:0/0:0), LPA(16:0/0:0), LPA (17:0/0:0), LPC(18:0/0:0), and LPC(18:1/0:0). The following compounds were purchased from Sigma-Aldrich Chemie GmbH: heptadecanoic acid, FAME Mix C4-C24 Unsaturates. Anhydrous organic solvents and inorganic reagents of the best available grade were purchased from Merck KGaA.

Plasma metabolomics by UPLC-ESI-QTOFMS

Serum samples were diluted with 20 volumes of 66% aqueous acetonitrile containing a single deuterated internal standard, [$^2H_{35}$]1-stearoyl-*sn*-glycero-3-phosphocholine (18:0-d_{35} LPC; 5 μmol/L), and analyzed as described previously (24).

Peak alignment, data deconvolution, and random forests analysis

The raw chromatographic and spectral data were aligned, deconvoluted, and normalized (summing the total ion current to 10,000) with MarkerLynx software (Waters). A total of 1,393 features were exported from MarkerLynx. Each spectral feature was represented by a unique m/z, retention time, and peak area. PCA and PLS-DA were conducted with the SIMCA P12+ software (Umetrics) to obtain an overview of the complete data set by unsupervised (PCA) and supervised (PLS-DA) methods. Data were normalized by Pareto scaling. The random forests machine learning algorithm as previously described (25) was used to classify serum samples as either HCC or 1 of the 3 control groups—AML, HV, or LC. This algorithm was chosen because it may be a more sensitive classifier (26). For the random forests analysis, age and sex were also included in the data matrix to evaluate their importance in discriminating between the 4 study groups.

Lipid profiling for LPCs in plasma by UPLC-ESI-TQMS

Plasma samples were prepared and chromatographed by UPLC as described earlier. The eluant was introduced by electrospray ionization in a triple quadrupole mass spectrometer (Waters Xevo TQ). LPCs were detected by multiple reaction monitoring (MRM). The LPCs and their respective MRMs are as follows: 14:0 (468 → 184, 104), 16:0 (496 → 184, 104), 16:1 (494 → 184, 104), 18:0 (524 → 184, 104), 18:0-d_{35} (559 → 184, 104), 18:1 (522 → 184, 104), 18:2 (520 → 184, 104), 18:3 (518 → 184, 104), and 20:4 (544 → 184, 104). TargetLynx was used for targeted quantitation.

Lipid profiling for LPA(16:0) in plasma by UPLC-ESI-TQMS

LPA(16:0) was profiled by modification of a previously described method (27). Briefly, plasma samples were diluted 1:10 with a buffer (50 μmol/L ammonium acetate with 0.5% trimethylamine and 90% methanol), centrifuged at 4°C to remove precipitated protein and other debris, and the supernatants transferred to autosampler vials. Samples were analyzed on a Xevo TQ mass spectrometer. LPA(17:0) was used as an internal standard. MRMs were as follows: LPA(16:0) 409 → 153 and LPA(17:0) 423 → 153. TargetLynx was used for targeted quantitation.

Lipid profiling for free and esterified fatty acids in plasma by GC-MS

Frozen samples were defrosted at ambient temperature, vortex mixed, and placed on ice. The entire sample preparation was carried out under nitrogen, and all solvents and solutions were degassed before use. For the analysis of free and esterified fatty acids, plasma samples were analyzed in triplicate with 3 independent sample preparations. Plasma (100 μL) was combined in 10-mL glass tubes with internal standard solution (100 μL) composed of heptadecanoic acid (200 μg/mL in hexane containing 0.01% BHT), vortex mixed for 5 seconds, and then reduced to dryness under a gentle stream of nitrogen at room temperature. The residues were dissolved in a mixture of anhydrous methanol and toluene 2:1 (2.0 mL) containing BHT (0.01%) and the samples placed on ice. To this solution, ice-cold acetyl chloride (200 μL) was added slowly to avoid splashing. After vortex mixing for 10 seconds, the samples were transferred to 3-mL Reacti-Vials [Thermo Fisher Scientific (Schweiz) AG] and incubated for 1 hour at 100°C in a heating block. Thereafter, the samples were transferred to 10-mL screw top glass tubes after cooling to room temperature and combined slowly with 6% potassium carbonate solution (5 mL). After thorough vortex mixing for 1 minute, the solutions were centrifuged at 780 × g for 10 minutes at room temperature and the organic upper phase carefully transferred to clean glass tubes containing approximately 200 mg of anhydrous sodium sulfate to eliminate trace amounts of water. After 1 hour at room temperature and repeated brief vortex mixing, the samples were centrifuged at 780 × g for 5 minutes at room temperature and the solutions transferred to glass tubes and dried under a slow stream of nitrogen at 50°C. Thereafter, the residues were reconstituted in hexane (200 μL) containing BHT (0.01%), vortex mixed, then briefly centrifuged to spin down insoluble precipitates, and finally an aliquot transferred to autosampler vials and subjected to GC-MS analysis. The rest of the samples were stored at −80°C under nitrogen. Samples were analyzed by GC-MS as previously described (28). For quantitation of fatty acids, calibration curves were prepared with heptadecanoic acid as an internal standard (see the earlier text) and a fatty acid concentration range of 0 to 1,000 μmol/L. For all fatty acids, the calibration curves were linear in this range ($r > 0.99$) and with coefficients of variance in the range 1% to 4%.

Statistical analysis

Significances were determined by the Student *t* test or ANOVA with Bonferroni correction for multiple comparisons with GraphPad Prism (GraphPad Software Inc.).

Results

Plasma metabolomics by UPLC-ESI-QTOFMS and random forests analysis

UPLC-ESI-QTOFMS plasma analysis yielded PCA and PLS-DA scores plots (Fig. 1A and B, respectively) and multidimensional scaling plots from the random forests analysis for HCC versus HV (Fig. 1C), HCC versus LC (Fig. 1D), and HCC versus AML (Fig. 1E). In the PCA scores plot, it can be seen that the HV and AML controls cluster together and are separated from the HCC and LC groups, which also clustered together. This unsupervised PCA gives a view of the internal structure of the data and reveals that supervised analyses must be used to generate the maximum separation between the classes HCC versus HV, HCC versus LC, and HCC versus AML. PLS-DA, a supervised analysis tool, was chosen, and the scores plot is shown in Fig. 1B. Compared with PCA (Fig. 1A), a better clustering and separation of the 4 classes was obtained with PLS-DA, with some slight overlap remaining between HCC and LC (Fig. 1B). Supervised analysis using random forests yielded 100% classification accuracy for HCC versus HV (Fig. 1C), 96.3% classification accuracy for HCC versus LC (Fig. 1D), and 97.6% classification accuracy for HCC versus AML (Fig. 1E). A single patient with liver cirrhosis was misclassified as an HCC patient by random forests (Fig. 1D). It is of considerable interest to note that this patient with liver cirrhosis was the only one with a Child–Pugh score of 10 (see Table 1), whereas all other patients with liver cirrhosis had a score of 5. It is possible that this patient, with metabolomic hallmarks closer to HCC than LC, was in transition to HCC. In addition, a single HCC patient was classified as an AML patient by random forests (Fig. 1E). No explanation is offered for this observation.

Random forests analysis produced a ranked list of ions responsible for the separation between each class of samples analyzed. It should be noted that PLS-DA identified similar metabolites as the random forests analysis (Supplementary Fig. S1). The principal upregulated and downregulated plasma markers in HCC versus each of the 3 control groups, AML, LC, and HV, are presented in Table 2. It is noteworthy that age and gender did not influence the results because after their inclusion in the random forests analysis, neither of these variables appeared in the top 100 variables (data not shown) identified in any of the comparisons described later.

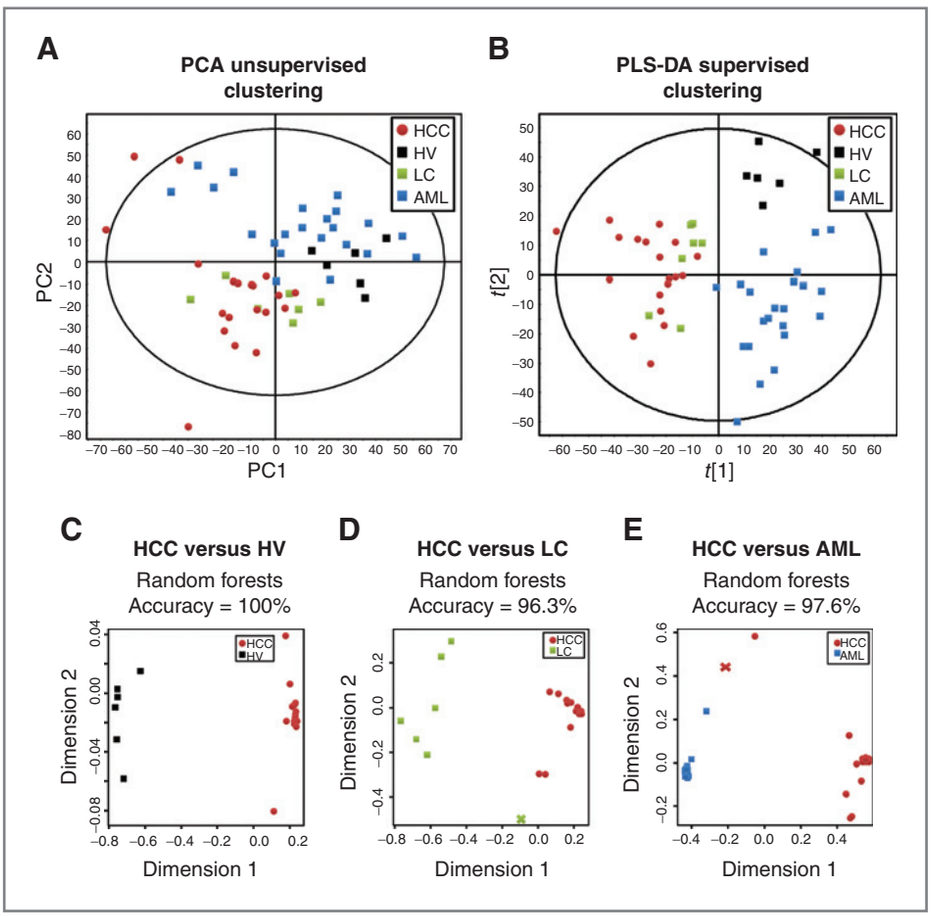

Figure 1. Multivariate data and random forests analyses of ions from HCC plasmas and 3 control groups. A, PCA showing clustering and partial resolution of the 4 study groups. B, PLS-DA showing improved clustering and resolution of the 4 study groups. C, separation by random forests analysis of HCC and HV with 100% classification accuracy. D, separation of HCC and LC by random forests analysis with 96.3% classification accuracy. E, separation of HCC and AML patients by random forests analysis with 97.6% classification accuracy. D, the cross sign represents misclassified LC. E, the cross sign represents misclassified HCC.

Table 2. Summary of upregulated and downregulated plasma metabolomic markers of HCC

Molecular changes	Identification status	Quantified	Comparator group		
			AML	LC	HV
LPC(14:0)	Tandem MS	TQMS		↓	↓
LPC(16:0)	Tandem MS w/standard	TQMS	↓		↓
LPC(18:0)	Tandem MS w/standard	TQMS	↓		↓
LPC(18:1)	Tandem MS w/standard	TQMS			↓
LPC(18:2)	Tandem MS	TQMS			↓
LPC(18:3)	Tandem MS	TQMS	↓		↓
LPC(20:4)	Tandem MS	TQMS			↓
LPC(24:0)	Tandem MS w/standard	TQMS			↑
FA(24:0)	Tandem MS w/standard	GC-MS		↓	↓
FA(24:1)	Tandem MS w/standard	GC-MS		↓	↓
Bilirubin	Accurate mass (*m/z*)	Clinical chemistry	↑	↑	
LPC(20:2)	Accurate mass (*m/z*)				↓
LPC(20:3)	Accurate mass (*m/z*)			↓	↓
LPC(20:5)	Accurate mass (*m/z*)				↓
LPC(22:6)	Accurate mass (*m/z*)			↓	
Biliverdin	Accurate mass (*m/z*)			↑	
7α-Hydroxy-3-oxochol-4-en-24-oic acid	Accurate mass (*m/z*)		↑		
3-Oxachola-4,6-dien-24-oic acid	Accurate mass (*m/z*)		↑		
Glycodeoxycholic acid	Tandem MS w/standard				↑
Deoxycholic acid 3-sulfate	Tandem MS				↑

Abbreviations: ↑, upregulated; ↓, downregulated; MS, mass spectrometry.

Hepatocellular carcinoma versus acute myelogenous leukemia. The AML control group was chosen because it represented a large tumor cell mass that probably had little direct influence upon hepatic metabolism. Their LFTs were, in general, within normal ranges (Table 1).

Two 3-oxo-Δ^4 bile acids, which are intermediates in the synthesis of chenodeoxycholic acid from cholesterol and generally considered to be fetal bile acids (29–33), 7α-hydroxy-3-oxochol-4-en-24-oic acid and 3-oxochola-4,6-dien-24-oic acid, were upregulated in HCC relative to AML (Table 2). On the basis of ion intensity, both of these bile acids were upregulated approximately 4-fold in HCC plasma relative to AML plasma. In addition, 3 LPCs, LPC(16:0), LPC(18:0), and LPC(18:3), were downregulated in HCC versus AML. Bilirubin was also upregulated in HCC relative to AML plasma (Table 2), and this is confirmed by clinical chemistry data in Table 1 ($t = 3.24$; $P = 0.0024$).

Hepatocellular carcinoma versus liver cirrhosis. The LC control group was chosen because all but one of the HCC tumors occurred within a cirrhotic liver (Table 1) and it was important to determine metabolomic markers that were associated with HCC rather than the underlying cirrhosis. Two unconjugated heme pigment metabolites, bilirubin and biliverdin, were upregulated in HCC relative to LC plasma. Based purely upon ion intensity, unconjugated bilirubin was approximately 3-fold upregulated and unconjugated biliverdin was approximately 10-fold upregulated. In addition, 3 downregulated LPCs, LPC(14:0), LPC(20:3), and LPC(22:6), were found for this comparison of patient classes by random forests. On the basis of ion intensity, these LPCs were downregulated in HCC versus LC plasma between 2- and 10-fold.

Hepatocellular carcinoma versus healthy volunteers. The control group HV was chosen in an attempt to uncover metabolomic markers that separated health from disease. Two conjugates of the bile acid deoxycholic acid, namely, glycodeoxycholic acid and deoxycholic acid 3-sulfate, were highly upregulated in HCC plasma relative to HV plasma. Based purely upon ion intensity, this upregulation was of the order of 30- to 50-fold. In addition, 7 LPCs, LPC(14:0), LPC (16:0), LPC(18:1), LPC(20:2), LPC(20:3), LPC(20:4), and LPC (20:5), were downregulated in HCC plasma relative to HV plasma (Table 2). Based upon ion intensity, the extent of downregulation of these ions in HCC plasma versus HV plasma was between 2- and 10-fold.

Metabolite profiling for plasma LPCs by UPLC-ESI-TQMS

Because of the consistent pattern of downregulated LPCs in HCC plasma observed earlier, it was decided to determine individual LPC plasma concentrations in all samples by UPLC-ESI-TQMS. Eight LPCs were determined by this method, and the findings are shown in Fig. 2. No correlations between any of the quantitated LPCs and the Child–Pugh scores were found in either the HCC or LC groups, separately or combined.

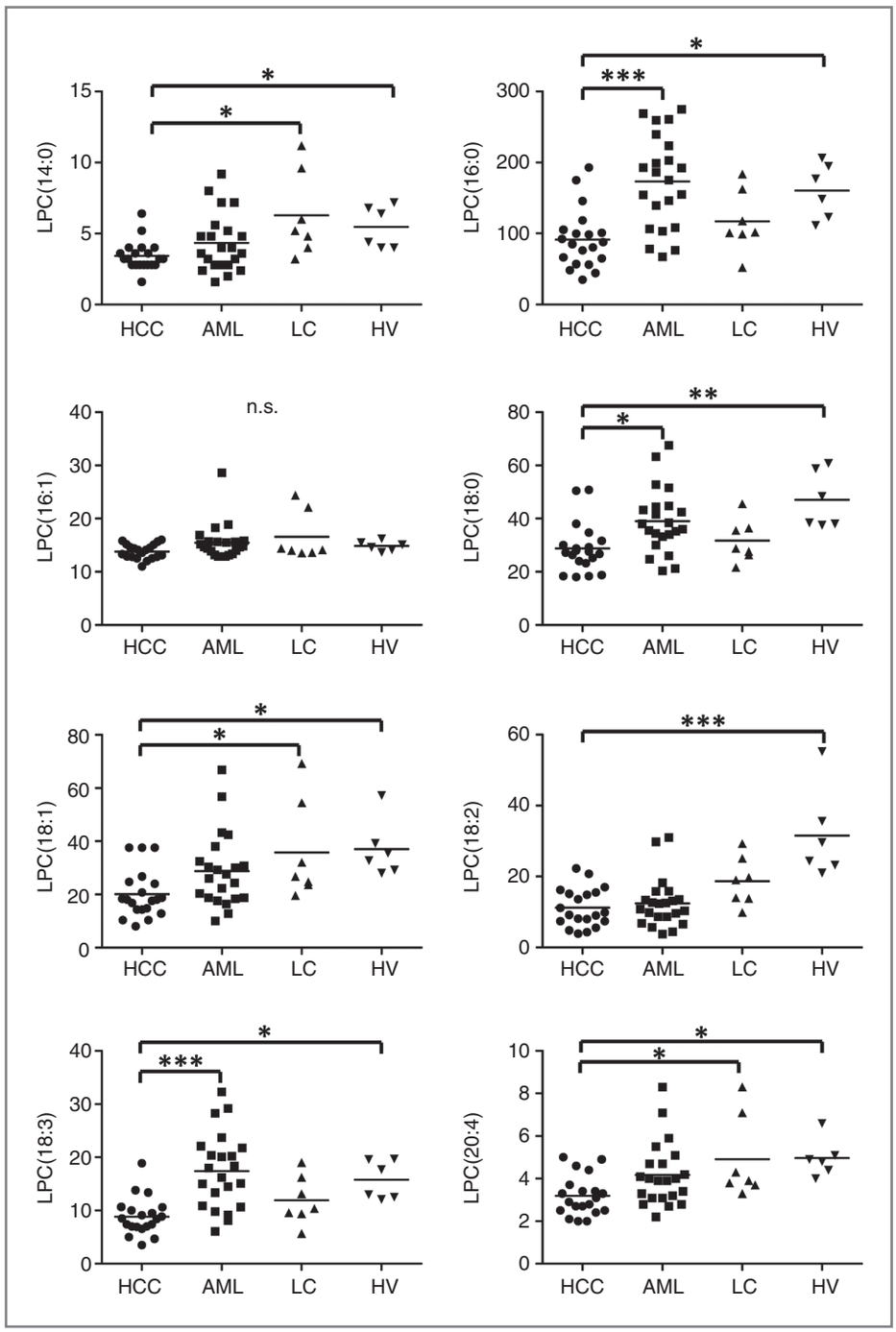

Figure 2. Plasma concentrations of 8 LPCs in HCC and 3 control groups. Plasma concentrations are expressed in micromoles per liter. HCC (20 cases), AML (22 cases), LC (7 cases), HV (6 subjects). Horizontal lines represent group means. Because of unequal variances, the nonparametric Kruskal–Wallis test was used with the Dunn multiple comparisons test. Levels of statistical significance are as follows: *, $P < 0.05$; **, $P < 0.01$; ***, $P < 0.001$. n.s., $P > 0.05$.

The aforementioned metabolomic study had indicated that LPC(14:0) was downregulated in HCC versus LC plasma, and the profiling study confirmed this and also showed that this LPC was downregulated in HCC versus HV plasma (Fig. 2). A negative correlation with AST ($P < 0.05$) was identified by the Pearson correlation analysis. LPC profiling revealed statistically significant downregulation of LPC(16:0) in HCC plasma relative to AML ($P < 0.001$) and HV ($P < 0.05$) plasma. When the metabolomic and profiling data were considered together, LPC(16:0) was downregulated in HCC plasma relative to plasma of both AML and HV control groups. The mean concentrations of LPC(16:1) were similar and tightly grouped in each study group and showed no statistically significant differences. The concentration of LPC(18:0) in HCC plasma was significantly ($P < 0.05$) lower than in AML plasma and very significantly ($P < 0.01$) lower than in HV plasma, using

stringent statistical evaluation. LPC(18:1) in HCC plasma showed a statistically significant ($P < 0.05$) lower plasma concentration than in HV plasma determined in this quantitative assay and also a statistically significant ($P < 0.05$) downregulation in HCC relative to LC. The plasma concentration of LPC(18:2) in HCC was highly statistically significantly ($P < 0.001$) lower in HCC than in HV controls. A negative correlation with ALT ($P < 0.05$) was identified by the Pearson correlation analysis. The plasma concentration of LPC(18:3) in HCC controls was highly significantly ($P < 0.001$) lower in HCC controls than in AML controls and significantly ($P < 0.05$) lower than in HV controls. The plasma concentration of LPC(20:4) in HCC controls was statistically significantly lower than in HV controls ($P < 0.05$) and in LC controls ($P < 0.05$).

Overall findings on LPCs by UPLC-ESI-TQMS. For 7 of the 8 LPCs measured, plasma levels in HCC controls were lower than in HV controls. For 3 of the 8 LPCs, the HCC plasma levels were lower than the plasma levels of both LC and AML controls.

Metabolite profiling for plasma fatty acids by GC-MS

Because of the provocative findings of lower LPCs in HCC plasma, it was decided to profile the total fatty acid concentration of the same plasma samples by GC-MS. The analytic method used methylated free fatty acids and transesterified fatty acid esters such as mono-, di-, and triglycerides so that the total fatty acid content of plasma, free and esterified can be determined (34). A total of 13 fatty acids were determined in plasma by GC-MS, with concentrations in micromoles per liter derived from calibration curves, using heptadecanoic acid [FA(17:0)] as an internal standard. The coefficients of variation for the determination of these fatty acids by GC-MS were all in the range 1% to 4%. Their mean ± SD concentrations in HCC plasma versus AML, LC, and HV plasma are given in Supplementary Table S1, whereas the concentrations for lignoceric acid [FA(24:0)] and nervonic acid [FA(24:1)] are shown in Fig. 3A.

Tetracosanoic acid (lignoceric acid, 24:0). The plasma concentration in HCC was virtually zero for all patients and showed a very statistically significantly ($P < 0.01$) lower concentration than in LC plasma and a highly statistically significantly ($P < 0.001$) concentration than in HV plasma. Remarkably, the AML plasma concentrations were similarly exhausted (Fig. 3A).

Tetracosenoic acid (nervonic acid, 24:1). Similar to its unsaturated counterpart lignoceric acid, this fatty acid was virtually absent from all HCC and AML plasmas. The plasma concentration of nervonic acid in HCC was very statistically significantly ($P < 0.01$) lower than LC plasma and highly statistically significantly ($P < 0.001$) below the concentration in HV plasma.

Overall findings on fatty acids by GC-MS. Of the 13 fatty acids profiled in plasma by GC-MS, 5 [FA(15:0), FA(20:4), FA (22:6), FA(24:0), and FA(24:1)] showed lower plasma concentrations in HCC than in certain controls (Supplementary Table S1; Fig. 3A). The most interesting finding to emerge from the fatty acid profiling of HCC and control plasma was the highly statistically significant quenching of the 2 very long-chain fatty acids (VLCFA) lignoceric acid (24:0) and nervonic acid (24:1). These very low levels in plasma may be due to enhanced peroxisomal β-oxidation of VLCFAs under the control of the peroxisome proliferator activated receptor alpha (PPARα) and as a result of either enhanced lignoceryl-CoA ligase activity (35) or activation of liver X receptor α (LXRα; ref. 36). There is evidence that PPARα is upregulated and related to the etiology of HCC in model systems (37, 38). This concept was therefore further examined in these patient samples. There is also evidence that LXRα activation may be involved in both HBV and HCV lipogenesis and hepatocarcinogenesis (39, 40).

Profiling for LPC(24:0) by UPLC-ESI-TQMS

Because of the aforementioned observations of very low 24:0 and 24:1 fatty acids in HCC and AML, it was decided to profile the corresponding LPC of 24:0, LPC(24:0), by UPLC-ESI-TQMS. Figure 3B shows the plasma concentrations in micromoles per liter for this low abundance LPC. Of considerable interest was the finding that HCC plasma displayed a statistically significant ($P < 0.05$) elevated concentration compared with HV plasma. This suggests that the prior findings were due to the free and esterified fatty acid compartment and not the phospholipid fraction.

Profiling for LPA(16:0) by UPLC-ESI-TQMS

Reduced levels of circulating LPCs may be due to their enhanced conversion by extracellular lysophospholipase D [LPD; autotoxin (ATX)] to LPAs (41). To test this hypothesis, we profiled LPA(16:0) concentrations in HCC and control plasma by UPLC-ESI-TQMS (27). The distribution of LPA (16:0) plasma concentrations in the 4 study groups is shown in Fig. 3C. All groups had similar levels, except for 4 HCC samples that displayed 5 to 10 times higher concentration. Inspection of the data set failed to reveal a common etiologic path for these 4 subjects, each having different predisposing factors. However, it was noted that these 4 patients had very high AFP concentrations. Both parametric linear regression and nonparametric Spearman rank correlation showed that LPA(16:0) levels and AFP concentrations were significantly well correlated ($r = 0.60$; $P = 0.005$; Fig. 3D).

Evidence for a role of PPARα in HCC from clinical plasma data

If PPARα is activated specifically in the livers of HCC patients relative to patients with liver cirrhosis and healthy volunteers, one would expect to observe in those former patients a decline in plasma uric acid, triglyceride, low-density lipoprotein cholesterol, and perhaps total cholesterol, levels accompanied by an increase in high-density lipoprotein cholesterol level (25). Supplementary Figure S2 shows no evidence for the activation of PPARα in these HCC patients relative to the control groups. It is therefore likely that if PPARα plays a role in these HCC cases, it does so directly, for example, by upregulating peroxisomal lignoceryl-CoA ligase activity (35).

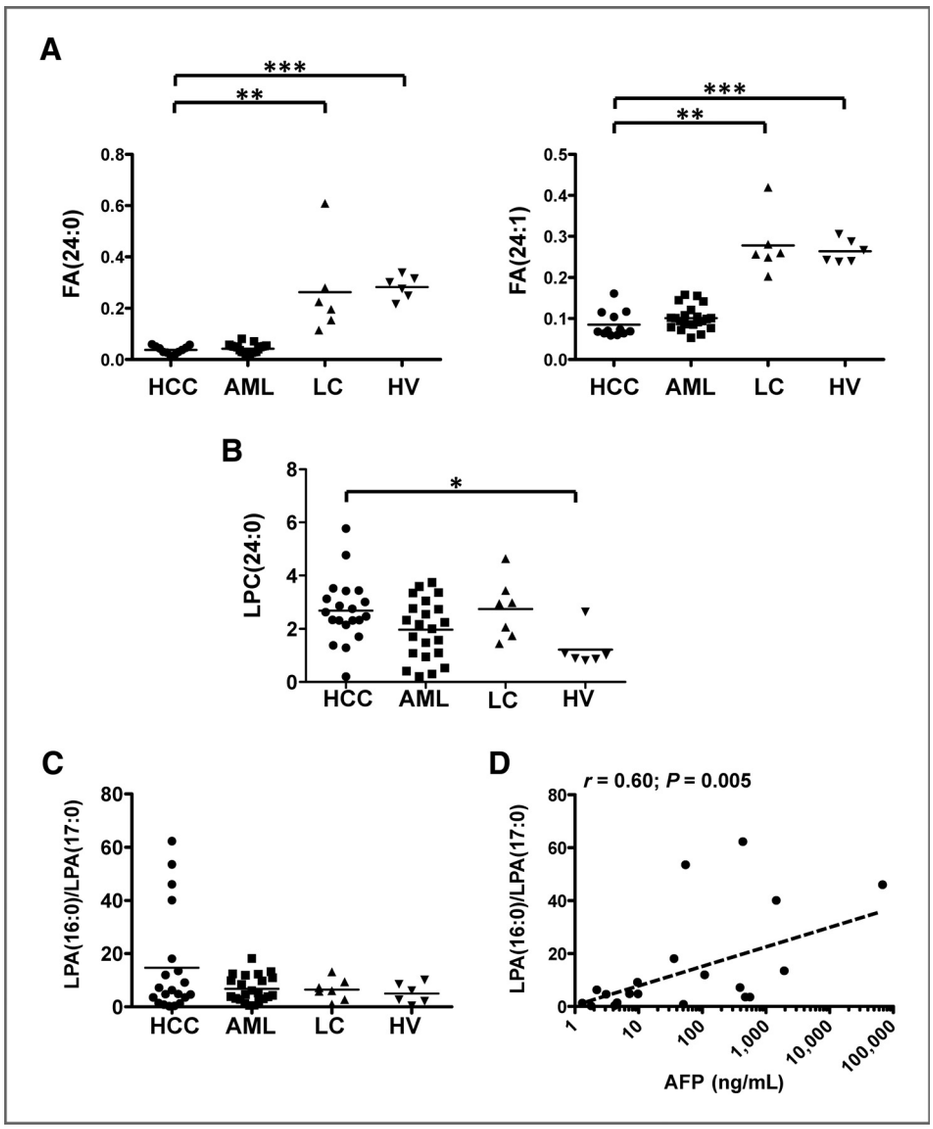

Figure 3. Results of lipid profiling by TQMS and GC-MS for selected fatty acids, LPCs, and LPAs. A, concentrations (μmol/L) of lignoceric acid [FA(24:0)] and nervonic acid [FA(24:1)] in HCC (20 cases), AML (22 cases), LC (7 cases), and HVs (6 subjects). Horizontal lines represent group means. Because of unequal variances, the nonparametric Kruskal–Wallis test was used with the Dunn multiple comparisons test. Levels of statistical significance are as follows: *, $P < 0.05$; **, $P < 0.01$; ***, $P < 0.001$. B, concentration (μmol/L) of LPC(24:0). C, relative concentration [normalized against internal standard LPA(17:0)] of LPA(16:0) in HCC, AML, LC, and HV. D, correlation between AFP plasma concentration (log ng/mL) and relative plasma concentration of LPA(16:0) in 20 cases of HCC.

Overall pattern of upregulated and downregulated molecules in HCC patients

A summary of the total molecular profile identified in HCC patients by metabolomic and lipid profiling procedures is given in Table 2. Perusal of this table reveals that there are no upregulated or downregulated molecules that are common to all 3 comparator groups (HV, LC, and AML). There are 7 molecules downregulated with respect to 2 comparator classes, 5 LPCs and 2 fatty acids. The perturbations in bile acid disposition (bile acid conjugates relative to HV) and fetal bile acids (relative to AML) are of interest because the 2 comparator groups involved (AML and HV) are the 2 groups without liver disease. In addition, bilirubin was found to be elevated in HCC plasma compared with AML and LC plasma and biliverdin in HCC plasma compared with LC plasma only.

The most obvious change in small plasma molecules was displayed by the 2 fatty acids, lignoceric acid (24:0) and nervonic acid (24:1), which were virtually exhausted in plasma of both HCC and AML controls. Whether these molecules are similarly reduced in the plasma of other patients with cancer is beyond the scope of this article.

Discussion

Metabolomic analysis of intermediate stage HCC (23), using plasma and UPLC-ESI-QTOFMS–based metabolomic protocols and random forests machine learning algorithm (26, 42), was used for the identification of metabolic intermediates in plasma that are altered in HCC. These studies were augmented by metabolite profiling for LPC and LPA by UPLC-ESI-TQMS and fatty acids by GC-MS. The accumulated data were analyzed by nonparametric statistics and tests for multiple comparisons. This stringency was thought to eliminate spurious metabolomic findings. Three comparator groups were

used, and random forests readily clustered and classified HCC from each comparator group. Healthy volunteers and AML patients were taken as control groups with no liver disease. Liver dysfunction is a rare complication of AML (43) and in a study of AML and acute lymphoblastic leukemia in Nepal (44), abnormal LFTs were recorded in a subset of the patients. LFTs were within normal ranges for the 22 AML patients described in this study.

The principal issue that needs to be addressed is what do these small molecules that are either elevated and attenuated in plasma of HCC patients teach us about HCC? It is pertinent to first examine their potential origins to gain more insights into what mechanisms may be at play in HCC. The 6 main findings of this study in relation to HCC versus controls are as follows: (1) 2 bile acid conjugates and 2 fetal bile acids were elevated, (2) bilirubin and biliverdin were elevated, (3) 11 lysophospholipids were attenuated, (4) 2 very long-chain fatty acids were attenuated, (5) LPA(16:0) was considerably elevated in 4 of 20 HCC patients, and (6) in the HCC group as a whole LPA(16:0) was strongly correlated with plasma AFP concentration.

For bile acid homeostasis, an early study recognized that fasting serum glycocholate concentrations were elevated in most patients with liver disease, but especially in LC (97.1% of cases) and HCC (94.7%; ref. 45). Overall, the literature provides a basis for the observation of elevated bile acid conjugates in HCC in this study. For the elevated plasma levels of 7α-hydroxy-3-oxochol-4-en-24-oic acid and 3-oxochol-4,6-dien-24-oic acid, these are the so-called 3-oxo-Δ^4 bile acids (30, 33) that are rarely encountered in the plasma of adults and usually considered to be fetal bile acids (33) that spill over into the urine in infants with cholestatic disease (30). There is a report that these bile acids are increased in both plasma and urine of HCC patients (33), where it was proposed that the appearance of fetal bile acids in the serum of HCC patients is the result of a metabolic process in the liver rather than cholestasis (33).

The largest number of molecules of interest that were altered in the plasma of HCC patients was in the phospholipid group of LPCs. A total of 11 LPCs were attenuated in HCC plasma. This finding strongly suggests that liver cirrhosis contributes greatly to the decline in LPCs in HCC plasma. As mentioned earlier, this interpretation is supported by the work of Yin and colleagues (21), whereby HCC- and HBV-induced liver cirrhosis shared a common decline in 4 LPCs, 3 of which, LPC(18:0), LPC(18:2), and LPC(18:3), are reported in this study. LPCs are metabolized by phospholipase D, generating LPAs, potent mitogens that act through LPA1-5 receptors (46). LPAs are also produced from LPCs extracellularly by LPD first described in rat plasma and that converted polyunsaturated LPCs to their saturated LPA counterparts (47). In the preceding 25 years, LPD has been shown to be identical to ATX and that ATX is strongly suspected of being involved in hepatocarcinogenesis (41). It was therefore decided to profile the HCC and control plasma levels for LPA(16:0), a product of LPD/ATX. Indeed, 4 of 20 HCC patients had inordinately high LPA(16:0) plasma levels and that LPA(16:0) strongly correlated with plasma AFP concentrations. It is of interest to note that both LPA (41) and AFP (48) may play a role in progression of HCC.

Two VLCFAs, lignoceric acid (24:0) and nervonic acid (24:1), were virtually exhausted in plasma of both HCC and AML controls. Lignoceric acid underwent a 7.5-fold decline in HCC plasma relative to LC plasma ($P < 0.01$). Similarly, nervonic acid decreased 3.4-fold in HCC plasma relative to LC plasma ($P < 0.001$). Note that, in both cases, plasma levels in HV controls were similar to those in LC controls. Whether or not other malignancies share this phenomenon with HCC and AML is not known and beyond the scope of this article.

In conclusion, we have undertaken a plasma metabolomic study of HCC, in which control groups of healthy volunteers, patients with liver cirrhosis, and AML patients were used. Upregulated molecules of interest in HCC included 2 conjugated bile acids, 2 bile pigments, and 2 fetal 3-oxo-Δ^4 bile acids. Downregulated molecules of interest included 11 LPCS and 2 VLCFAs, lignoceric acid and nervonic acid. All these molecular changes in the plasma of HCC patients provide new insights into the pathobiology of the disease.

Disclosure of Potential Conflicts of Interest

No potential conflicts of interest were disclosed.

Grant Support

This work was supported by NIH, National Cancer Institute Intramural Research Program (A.D. Patterson, K.W. Krausz, and F.J. Gonzalez), NIH grants U19 AI067773-05/-06 (NIAID; C. Lanz and J.R. Idle) and U01 ES016013 (NIEHS; A.D. Patterson, K.W. Krausz, and F.J. Gonzalez), and Bernerische und Schweizerische Krebsliga, Sasella Foundation, and the Hassan Badawi Foundation Against Liver Cancer (O. Maurhofer, J.R. Idle, and J-F. Dufour).

The costs of publication of this article were defrayed in part by the payment of page charges. This article must therefore be hereby marked *advertisement* in accordance with 18 U.S.C. Section 1734 solely to indicate this fact.

Received March 14, 2011; revised August 30, 2011; accepted August 30, 2011; published OnlineFirst September 7, 2011.

References

1. Llovet JM, Burroughs A, Bruix J. Hepatocellular carcinoma. Lancet 2003;362:1907–17.
2. Pei Y, Zhang T, Renault V, Zhang X. An overview of hepatocellular carcinoma study by omics-based methods. Acta Biochim Biophys Sin (Shanghai) 2009;41:1–15.
3. Wang XW, Thorgeirsson SS. Transcriptome analysis of liver cancer: ready for the clinic?J Hepatol 2009;50:1062–4.
4. Boyault S, Rickman DS, de Reynies A, Balabaud C, Rebouissou S, Jeannot E, et al. Transcriptome classification of HCC is related to gene alterations and to new therapeutic targets. Hepatology 2007;45:42–52.
5. Iizuka N, Oka M, Yamada-Okabe H, Mori N, Tamesa T, Okada T, et al. Comparison of gene expression profiles between hepatitis B virus- and hepatitis C virus-infected hepatocellular carcinoma by oligonucleotide microarray data on the basis of a supervised learning method. Cancer Res 2002;62:3939–44.
6. Okabe H, Satoh S, Kato T, Kitahara O, Yanagawa R, Yamaoka Y, et al. Genome-wide analysis of gene expression in human hepatocellular

carcinomas using cDNA microarray: identification of genes involved in viral carcinogenesis and tumor progression. Cancer Res 2001;61: 2129–37.
7. Wurmbach E, Chen YB, Khitrov G, Zhang W, Roayaie S, Schwartz M, et al. Genome-wide molecular profiles of HCV-induced dysplasia and hepatocellular carcinoma. Hepatology 2007;45:938–47.
8. Delpuech O, Trabut JB, Carnot F, Feuillard J, Brechot C, Kremsdorf D. Identification, using cDNA macroarray analysis, of distinct gene expression profiles associated with pathological and virological features of hepatocellular carcinoma. Oncogene 2002;21:2926–37.
9. De Giorgi V, Monaco A, Worchech A, Tornesello M, Izzo F, Buonaguro L, et al. Gene profiling, biomarkers and pathways characterizing HCV-related hepatocellular carcinoma. J Transl Med 2009;7:85.
10. Lee JSChu IS, Mikaelyan A, Calvisi DF, Heo J, Reddy JK, et al. Application of comparative functional genomics to identify best-fit mouse models to study human cancer. Nat Genet 2004;36: 1306–11.
11. Idle JR, Gonzalez FJ. Metabolomics. Cell Metab 2007;6:348–51.
12. Patterson AD, Lanz C, Gonzalez FJ, Idle JR. The role of mass spectrometry-based metabolomics in medical countermeasures against radiation. Mass Spectrom Rev 2010;29:503–21.
13. Dettmer K, Aronov PA, Hammock BD. Mass spectrometry-based metabolomics. Mass Spectrom Rev 2007;26:51–78.
14. Mamas M, Dunn WB, Neyses L, Goodacre R. The role of metabolites and metabolomics in clinically applicable biomarkers of disease. Arch Toxicol 2011;85:5–17.
15. Johnson CH, Patterson AD, Krausz KW, Lanz C, Kang DW, Luecke H, et al. Radiation metabolomics. 4. UPLC-ESI-QTOFMS-based metabolomics for urinary biomarker discovery in gamma-irradiated rats. Radiat Res 2011;175:473–84.
16. Lanz C, Patterson AD, Slavik J, Krausz KW, Ledermann M, Gonzalez FJ, et al. Radiation metabolomics. 3. Biomarker discovery in the urine of gamma-irradiated rats using a simplified metabolomics protocol of gas chromatography-mass spectrometry combined with random forests machine learning algorithm. Radiat Res 2009; 172:198–212.
17. Patterson AD, Idle JR. A metabolomic perspective of small molecule toxicology. In:Ballantyne B, Marrs T, Syversen T, editors. General and applied toxicology. 3rd ed. Chichester, UK: John Wiley & Sons Ltd.; 2009. p. 439–65.
18. Manna SK, Patterson AD, Yang Q, Krausz KW, Li H, Idle JR, et al. Identification of noninvasive biomarkers for alcohol-induced liver disease using urinary metabolomics and the Ppara-null mouse. J Proteome Res 2010;9:4176–88.
19. Gao H, Lu Q, Liu X, Cong H, Zhao L, Wang H, et al. Application of ^{1}H NMR-based metabonomics in the study of metabolic profiling of human hepatocellular carcinoma and liver cirrhosis. Cancer Sci 2009;100:782–5.
20. Wu H, Xue R, Dong L, Liu T, Deng C, Zeng H, et al. Metabolomic profiling of human urine in hepatocellular carcinoma patients using gas chromatography/mass spectrometry. Anal Chim Acta 2009; 648:98–104.
21. Yin P, Wan D, Zhao C, Chen J, Zhao X, Wang W, et al. A metabonomic study of hepatitis B-induced liver cirrhosis and hepatocellular carcinoma by using RP-LC and HILIC coupled with mass spectrometry. Mol Biosyst 2009;5:868–76.
22. Bruix J, Sherman M, Llovet JM, Beaugrand M, Lencioni R, Burroughs AK, et al. Clinical management of hepatocellular carcinoma. Conclusions of the Barcelona-2000 EASL conference. European Association for the Study of the Liver. J Hepatol 2001;35:421–30.
23. Pons F, Varela M, Llovet JM. Staging systems in hepatocellular carcinoma. HPB (Oxford) 2005;7:35–41.
24. Chen C, Shah YM, Morimura K, Krausz KW, Miyazaki M, Richardson TA, et al. Metabolomics reveals that hepatic stearoyl-CoA desaturase 1 downregulation exacerbates inflammation and acute colitis. Cell Metab 2008;7:135–47.
25. Patterson AD, Slanar O, Krausz KW, Li F, Hofer CC, Perlik F, et al. Human urinary metabolomic profile of PPARalpha induced fatty acid beta-oxidation. J Proteome Res 2009;8:4293–300.
26. Breiman L. Random forests. Mach Learn 2001;45:5–32.
27. Aaltonen N, Laitinen JT, Lehtonen M. Quantification of lysophosphatidic acids in rat brain tissue by liquid chromatography-electrospray tandem mass spectrometry. J Chromatogr B Analyt Technol Biomed Life Sci 2010;878:1145–52.
28. Lanz C, Ledermann M, Slavik J, Idle JR. The production and composition of rat sebum is unaffected by 3 Gy gamma radiation. Int J Radiat Biol 2011;87:360–71.
29. Ikawa S, Ayaki Y, Ogura M, Yamasaki K. The metabolism *in vivo* and *in vitro* of 3-oxo-7-hydroxychol-4-enoic acid-24-14 C as an intermediate of chenodeoxycholic acid biogenesis. J Biochem 1972; 71:579–87.
30. Kimura A, Suzuki M, Murai T, Kurosawa T, Tohma M, Sata M, et al. Urinary 7alpha-hydroxy-3-oxochol-4-en-24-oic and 3-oxochola-4,6-dien-24-oic acids in infants with cholestasis. J Hepatol 1998;28: 270–9.
31. Ogundare M, Theofilopoulos S, Lockhart A, Hall LJ, Arenas E, Sjovall J, et al. Cerebrospinal fluid steroidomics: are bioactive bile acids present in brain?J Biol Chem 2010;285:4666–79.
32. Yoshimura T, Taniguchi T, Kobayashi D, Komiya T, Murai T, Kimura A, et al. Enzyme immunoassay for conjugated 7alpha-hydroxy-3-oxo-4-cholenoic acid in human urine. J Immunoassay Immunochem 2001; 22:1–13.
33. El-Mir MY, Badia MD, Luengo N, Monte MJ, Marin JJ. Increased levels of typically fetal bile acid species in patients with hepatocellular carcinoma. Clin Sci 2001;100:499–508.
34. Wu X, Tong Y, Shankar K, Baumgardner JN, Kang J, Badeaux J, et al. Lipid fatty acid profile analyses in liver and serum in rats with nonalcoholic steatohepatitis using improved gas chromatography-mass spectrometry methodology. J Agric Food Chem 2011;59: 747–54.
35. Asayama K, Sandhir R, Sheikh FG, Hayashibe H, Nakane T, Singh I. Increased peroxisomal fatty acid beta-oxidation and enhanced expression of peroxisome proliferator-activated receptor-alpha in diabetic rat liver. Mol Cell Biochem 1999;194: 227–34.
36. Hu T, Foxworthy P, Siesky A, Ficorilli JV, Gao H, Li S, et al. Hepatic peroxisomal fatty acid beta-oxidation is regulated by liver X receptor alpha. Endocrinology 2005;146:5380–7.
37. Meyer K, Lee JS, Dyck PA, Cao WQ, Rao MS, Thorgeirsson SS, et al. Molecular profiling of hepatocellular carcinomas developing spontaneously in acyl-CoA oxidase deficient mice: comparison with liver tumors induced in wild-type mice by a peroxisome proliferator and a genotoxic carcinogen. Carcinogenesis 2003; 24:975–84.
38. Tanaka N, Moriya K, Kiyosawa K, Koike K, Aoyama T. Hepatitis C virus core protein induces spontaneous and persistent activation of peroxisome proliferator-activated receptor alpha in transgenic mice: implications for HCV-associated hepatocarcinogenesis. Int J Cancer 2008;122:124–31.
39. Moriishi K, Mochizuki R, Moriya K, Miyamoto H, Mori Y, Abe T, et al. Critical role of PA28gamma in hepatitis C virus-associated steatogenesis and hepatocarcinogenesis. Proc Natl Acad Sci U S A 2007;104: 1661–6.
40. Na TY, Shin YK, Roh KJ, Kang SA, Hong I, Oh SJ, et al. Liver X receptor mediates hepatitis B virus X protein-induced lipogenesis in hepatitis B virus-associated hepatocellular carcinoma. Hepatology 2009;49:1122–31.
41. Wu JM, Xu Y, Skill NJ, Sheng H, Zhao Z, Yu M, et al. Autotaxin expression and its connection with the TNF-alpha-NF-kappaB axis in human hepatocellular carcinoma. Mol Cancer 2010;9: 71.
42. Patterson AD, Li H, Eichler GS, Krausz KW, Weinstein JN, Fornace AJ Jr., et al. UPLC-ESI-TOFMS-based metabolomics and gene expression dynamics inspector self-organizing metabolomic maps as tools for understanding the cellular response to ionizing radiation. Anal Chem 2008;80:665–74.
43. Wandroo FA, Murray J, Mutimer D, Hubscher S. Acute myeloid leukaemia presenting as cholestatic hepatitis. J Clin Pathol 2004; 57:544–5.

44. Sharma Poudel B, Karki L. Abnormal hepatic function and splenomegaly on the newly diagnosed acute leukemia patients. JNMA J Nepal Med Assoc 2007;46:165–9.

45. Tanggo Y, Fujiyama S, Kin F, Tashiro A, Shiraoku H, Akahoshi M, et al. Clinical usefulness of serum cholylglycine determination in various liver diseases. Gastroenterol Jpn 1982;17:447–52.

46. Mutoh T, Chun J. Lysophospholipid activation of G protein-coupled receptors. Subcell Biochem 2008;49:269–97.

47. Tokumura A, Harada K, Fukuzawa K, Tsukatani H. Involvement of lysophospholipase D in the production of lysophosphatidic acid in rat plasma. Biochim Biophys Acta 1986;875:31–8.

48. McHugh PP, Gilbert J, Vera S, Koch A, Ranjan D, Gedaly R. Alpha-fetoprotein and tumour size are associated with microvascular invasion in explanted livers of patients undergoing transplantation with hepatocellular carcinoma. HPB (Oxford) 2010;12:56–61.